IEEE Access
Multidisciplinary | Rapid Review | Open Access Journal

Received May 8, 2017, accepted May 19, 2017, date of publication June 20, 2017, date of current version July 17, 2017.

Digital Object Identifier 10.1109/ACCESS.2017.2713802

A Joint Multiuser Detection Scheme for UWB Sensor Networks Using Waveform Division Multiple Access

ZHENDONG YIN[1], (Member, IEEE), MINGYANG WU[1], ZHUTIAN YANG[1], (Member, IEEE), NAN ZHAO[2], (Senior Member, IEEE), AND YUNFEI CHEN[3], (Senior Member, IEEE)

[1]School of Electronics and Information Engineering, Harbin Institute of Technology, Harbin, China
[2]School of Information and Communication Engineering, Dalian University of Technology, Dalian, China
[3]School of Engineering, University of Warwick, Coventry CV4 7AL, U.K.

Corresponding author: Zhendong Yin (yinzhendong@hit.edu.cn)

This work was supported by the National Natural Science Foundation of China under Grant 61471142, Grant 61102084, Grant 61601145, and Grant 61571167.

ABSTRACT A joint multiuser detection (MUD) scheme for wireless sensor networks (WSNs) is proposed to suppress multiple access interference (MAI) caused by a large number of sensor nodes. In WSNs, waveform division multiple access ultra-wideband (WDMA-UWB) technology is well suited for robust communications. Multiple sensor nodes are allowed to transmit modulated signals by sharing the same time periods and frequency bands using orthogonal pulse waveforms. This paper employs a mapping function based on the optimal multiuser detection to map the received bits into the mapping space where error bits can be distinguished. In order to revise error bits caused by MAI, the proposed joint MUD scheme combines the mapping function with suboptimal algorithms. Numerical results demonstrate that the proposed MUD scheme provides good performances in terms of suppressing MAI and resisting near-far effect with low computational complexity.

INDEX TERMS Joint algorithm, multiuser detection, mapping function, waveform division multiple access ultra-wideband, wireless sensor networks.

I. INTRODUCTION

Wireless sensor networks (WSNs) have gained tremendous attention in recent years due to the development of low-cost, low-power, smart sensors and the great importance in a wide variety of applications [1], [2]. The sensor nodes of WSNs transmit the collected information to the base station using reliable communication links between sensors [3]. Considering the requirements and constraints of the communications between sensors, such as the good real-time performance, good ability of robustness, variable data rate, low power consumption and high user capacity, the impulse radio ultra-wideband (IR-UWB) technology is suitable for WSNs. The applications of UWB-based WSNs include positioning [4], indoor navigation [5], safety monitoring [6], distributed detection [7], etc. However, for these application scenarios, the WSNs suffer from harsh multiple access interference (MAI) owing to the communications between sensor nodes in the same channels.

In order to overcome this problem, MAI suppression technologies have been applied to transmitters or receivers for UWB systems. At the transmitter, multiple access approaches are considered as the necessary modulation schemes. The traditional multiple access approaches for IR-UWB systems commonly include time hopping (TH) and direct sequence (DS) methods. Both multiple access approaches are similar to code division multiple access (CDMA) which exploits multiple access potential and user capacity of communication systems by applying different codes. In [8] and [9], a hybrid DS-TH-UWB system combines TH with DS to obtain the good performance in the multiuser environment.

At the receiver, multiuser detection (MUD) is an effective MAI suppression technology which has been considered in many studies. In [10], a combined ant colony MUD algorithm for DS-UWB systems was proposed which can decrease the complexity and improve the performance by applying biological optimization strategy to MUD problem. A MUD algorithm based on neural networks, approximating maximum likelihood functions by nonlinear methods, has the good detection performance, but with the disadvantages of higher complexity, lower convergent speed

and lack of theoretic analysis methods [11]. Some multiuser detectors based on intelligent optimization algorithms were also suggested in [12]–[14]. Reference [15] combined minimum mean square error (MMSE) algorithm with SIC algorithm to improve the performance of each algorithm. A MUD algorithm based on matched filter and identification of error bits was proposed in [16]. However, the pseudorandom code with the length of 255 used in the transmitter reduces the bit rate when the pulse cycle is assured. It was demonstrated in [17] that frequency-domain MMSE turbo equalization schemes can offer better tradeoff between the performance and the complexity for DS-UWB systems. Another technique to reduce MAI is to combine channel coding (such as LDPC codes) with MUD schemes which achieves a good BER performance and low energy consumption [18].

In order to suppress MAI in WSNs, we adopt waveform division multiple access ultra-wideband (WDMA-UWB) technology [19], [20], to establish wireless communication links between sensors, and propose a joint MUD scheme. The main contributions are stated as follows.

- We use Gegenbauer orthogonal polynomials to design UWB pulse waveforms and apply the WDMA-UWB scheme for suppressing MAI in transmitter. The multiple access is achieved by using different orthogonal pulse waveforms. Compared with TH-UWB and DS-UWB, WDMA-UWB has many unique advantages, for instance, high actual communication rate, simple synchronization acquisition process and uncomplicated transceivers.
- In this paper, a mapping-based MUD scheme is proposed for asynchronous UWB communication systems. Similar to TH-UWB and DS-UWB, WDMA-UWB systems also have MAI owing to the incomplete orthogonality of pulse waveforms. Furthermore, the near-far effect without power control can also affect the communications. We present a mapping function on the basis of the OMD solution to solve these problems. The mapping function maps the bits judged by matched filters to the mapping space.
- The joint MUD scheme is proposed which combines the mapping-based method with suboptimal MUD algorithms, such as the traditional matched filter (MF), decorrelation (DEC) and MMSE. We consider the output of the suboptimal multiuser detector as approximate information bits in order to calculate the boundaries for distinguishing error bits. The proposed MUD scheme is validated by computer simulation in an asynchronous WDMA-UWB system.

The rest of this paper is organized as follows. In Section II, we describe the model of the WDMA-UWB system, including the transmitter model, the establishment of WDMA-UWB communication links and the receiver model. In Section III, the principle and block diagram of the proposed joint MUD algorithm based on the optimal mapping function and suboptimal detectors are discussed. In Section IV, we present simulation results that compare with other MUD algorithms, followed by conclusions given in Section V.

II. SYSTEM MODEL

We consider an asynchronous K-node WSN based on the UWB system transmitting signal through dense multipath channels, where each user employs binary phase shift keying (BPSK) WDMA modulation.

A. TRANSMITTER MODEL

The transmitted signal of the kth user (where $k = 1, 2, , K$) can be expressed as

$$x_k(t) = \sum_{i=1}^{M} a_k d_k(i) w_k(t - iT_s), \tag{1}$$

where $d_k(i) \in \{-1, 1\}$ denotes the ith BPSK modulated symbol for the kth user, and M is the number of bits. Moreover a_k and T_s denote the amplitude value and repetition period of per pulse, respectively. In this paper, the UWB pulse denoted by $w_k(t)$ is depicted in Fig. 1. We design the orthogonal pulse waveforms by using Gegenbauer orthogonal polynomials to provide waveform division multiple access modes. The Gegenbauer orthogonal polynomials employed in [21] and [22] is given by

$$C_n^{(\gamma)}(x) = \sum_{k=0}^{\lfloor n/2 \rfloor} (-1)^k \frac{\Gamma(n-k+\gamma)}{\Gamma(\gamma)k!(n-2k)!}(2x)^{n-2k}. \tag{2}$$

The recursion formula of Gegenbauer orthogonal polynomials can be expressed as

$$\begin{cases} C_0^{\gamma}(x) = 1 \\ C_1^{\gamma}(x) = 2\gamma x \\ C_n^{\gamma}(x) = \frac{1}{n}[2x(n+\gamma-1)C_{n-1}^{\gamma}(x) - (n+\gamma-2)C_{n-2}^{\gamma}(x)]. \end{cases} \tag{3}$$

According to (3), the expression of Gegenbauer pulse waveforms is given by

$$w_k(t) = C_k^{\gamma}(t)\sqrt{h(t)}, \tag{4}$$

where $h(t)$ denotes the weight function of Gegenbauer polynomials.

The oscillation frequency of the time domain Gegenbauer pulse waveforms increases with the Gegenbauer polynomials' order. Therefore, it is obvious that the frequency spectrum bandwidth also increases with the order. If we generate nanosecond Gegenbauer pulses, the orthogonal pulses can be used for WDMA-UWB systems with GHz spectrum bandwidth. Due to the orthogonality of Gegenbauer pulses in synchronous UWB systems, the interference from other transmitters can be completely suppressed by using coherent receivers. However, the incomplete orthogonality of Gegenbauer pulse waveforms in asynchronous UWB systems causes the slight MAI which can be suppressed by MUD algorithms.

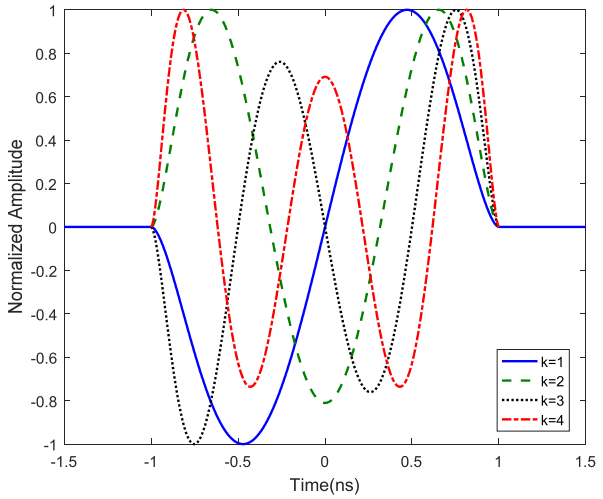

FIGURE 1. The pulse waveforms based on Gegenbauer orthogonal polynomials.

B. CHANNEL MODEL

The UWB channel model that we consider is the IEEE 802.15.4a standard channel model for the indoor WSNs environment [23]. The standard channel model is suitable for both low and high data rate short-range UWB systems. The channel impulse response of the standard channel model can be expressed as

$$h(t) = \sum_{u=0}^{L_c-1} \sum_{v=0}^{L_m-1} \alpha_{u,v} e^{j\phi_{u,v}} \delta\left(t - T_u - \tau_{u,v}\right), \tag{5}$$

where $\alpha_{u,v}$ is the amplitude coefficient of the vth multipath component in the uth cluster, and L_c and L_m denote the number of clusters and the number of multipath components in one cluster, respectively. $\phi_{u,v}$ denotes uniformly distributed random variable in $[0, 2\pi]$. T_u denotes the arrival time of the uth cluster. Furthermore, $\tau_{u,v}$ is the arrival time of the vth multipath component in the uth cluster. For simplicity, equation (5) can be expressed as

$$h(t) = \sum_{l=0}^{L-1} \alpha_l \delta\left(t - T_l\right), \tag{6}$$

where L, α_l and T_l denote the total number of multipath components, the amplitude coefficient and the arrival time of the lth multipath component, respectively.

C. RECEIVER MODEL

We consider RAKE receivers which employ the maximal-ratio combining (MRC) scheme in order to combine the signals obtained from different RAKE fingers. The impact of inter symbol interference (ISI) is so weak that ISI is not taken into consideration in this paper when the root-mean squared (RMS) delay spread is much lower than the UWB pulse rate. The received signal of the ith bit can be written as

$$r(t) = \sum_{k=1}^{K} a_k d_k(i) \sum_{l=1}^{L} \alpha_l w_k(t - \tau_k - T_l) + n(t), \tag{7}$$

where τ_k is the channel delay of kth user and $n(t)$ is zero-mean additive white Gaussian noise (AWGN) with two sided power spectral density $N_0/2$ W/Hz. For simplicity, we analyze the received signal in one symbol period T_s. The output of the pth RAKE receiver can be expressed by

$$\begin{aligned} y_p &= \sum_{j=1}^{L_R} c_j \int_{iT_s+\tau_p}^{(i+1)T_s+\tau_p} r(t) m_j(t) dt \\ &= a_p d_p(i) r_{pp} + \sum_{\substack{k=1 \\ k\neq p}}^{K} a_k d_k(i) r_{kp} + n_p, \end{aligned} \tag{8}$$

where c_j and L_R denote the weight coefficient according to MRC scheme and the number of RAKE fingers, respectively. $m_j(t)$ is the local template signal corresponding to the jth separable multipath which can be expressed by

$$m_j(t) = w_p(t - T_j - \tau_p). \tag{9}$$

Moreover, the correlation value r_{kp} with the influence of multipath is given by

$$r_{kp} = \sum_{l=1}^{L} \sum_{j=1}^{L_R} \alpha_l c_j \int_{T_s} w_k(t - \tau_k - T_l) w_p(t - \tau_p - T_j) dt. \tag{10}$$

The first term of (8) denotes the desired signal of the pth user, the second term denotes the MAI and the last term denotes the noise interference. The MAI term is caused by incomplete orthogonality of Gegenbauer pulse waveforms. If the UWB system builds completely synchronous communication links, the Gegenbauer pulse waveforms are orthogonal to each other which can suppress MAI thoroughly. However, the existence of MAI in asynchronous systems has a significant impact on the user capacity and the BER performance.

We assume that vector $\mathbf{y} = [y_1, y_2, \ldots, y_K]^{\mathrm{T}}$ denotes the output of the group of RAKE receivers and vector $\mathbf{b} = [b_1, b_2, \ldots, b_K]^{\mathrm{T}}$ denotes the output of sign detectors. Thus, $\mathbf{y}$ can be expressed as

$$\mathbf{y} = \mathbf{RAd} + \mathbf{n}, \tag{11}$$

$$\mathbf{b} = sgn(\mathbf{y}), \tag{12}$$

where the vector $\mathbf{d} = [d_1, d_2, \ldots, d_K]^{\mathrm{T}}$ denotes the real transmitted bits of each sensor node, the vector $\mathbf{n} = [n_1, n_2, \ldots, n_K]^{\mathrm{T}}$ denotes the noise interference. The matrix $\mathbf{R} = (r_{kp})_{K\times K}$ denotes the cross-correlation matrix and $\mathbf{A} = \mathrm{diag}(a_1, a_2, \ldots, a_K)$ is the amplitude matrix.

III. PROPOSED JOINT MULTIUSER DETECTION ALGORITHM

The OMD proposed by Verdu lays the theoretical foundation for MUD. The optimal solution to OMD is given by

$$\mathbf{b}_{\mathrm{OMD}} = \arg\{\max_{\mathbf{b}\in\{-1,+1\}} (2\mathbf{b}^{\mathbf{T}}\mathbf{Ay} - \mathbf{b}^{\mathbf{T}}\mathbf{ARAb})\}. \tag{13}$$

In this section, we employ a mapping function proposed in [18] based on OMD to develop the MUD algorithm. In order to solve the optimization problem, we assume that

$$F(\mathbf{b}) = \frac{1}{2}\mathbf{b^T ARAb} - \mathbf{b^T Ay}. \tag{14}$$

According to (13), the optimization problem of OMD can be transformed into the solution to $\mathbf{b}$ that minimizes the function $F(\mathbf{b})$. We can rewrite (14) as

$$F(\mathbf{b}) = \frac{1}{2}\sum_{i=1}^{K}\sum_{j=1}^{K} a_i a_j r_{ij} b_i b_j - \sum_{i=1}^{K} b_i a_i y_i. \tag{15}$$

The function $F(\mathbf{b})$ is a quadratic form about vector $\mathbf{b}$. In order to reduce the complexity of $F(\mathbf{b})$ and construct a mapping function, we calculate the derivative of $F(\mathbf{b})$ to decrease the order of function. The partial derivative of (14) can be expressed by

$$\frac{\partial F}{\partial \mathbf{b}} = \mathbf{ARAb} - \mathbf{Ay}. \tag{16}$$

Then, (16) can be further written as follows:

$$\begin{cases} \dfrac{\partial F}{\partial b_1} = \displaystyle\sum_{j=1}^{K} a_1 a_j r_{1j} b_j - a_1 y_1, \\ \dfrac{\partial F}{\partial b_2} = \displaystyle\sum_{j=1}^{K} a_2 a_j r_{2j} b_j - a_2 y_2, \\ \quad \cdots \\ \dfrac{\partial F}{\partial b_K} = \displaystyle\sum_{j=1}^{K} a_K a_j r_{Kj} b_j - a_K y_K. \end{cases} \tag{17}$$

Based on (17), we assume that the mapping function is

$$M(b_k) = \sum_{j=1}^{K} a_k a_j r_{kj} b_j - a_k y_k, \quad k = 1, 2, \ldots, K. \tag{18}$$

Note that there is a one-to-one correspondence between b_k and $M(b_k)$. It is obvious that $M(b_k)$ is a linear equation without complex computations. Thus, we regard $M(b_k)$ as a mapping function which can map b_k to the feature space.

The absolute mapping values of ten thousand received bits in the condition of 10 users at SNR = 10dB are shown in Fig. 2. It is obvious that the mapping values of error bits are generally higher than those of correct bits. Hence, we employ the mapping values to distinguish error bits. The error bits are caused by various interferences which can change the mapping value. MAI is an important interference factor with the exception of AWGN and multipath effect. The RAKE receivers and WDMA technique can effectively suppress the multipath effect. Thus, MAI is the main interference at high SNR. In order to find the boundaries between error bits and correct bits, we analyze the relation between $M(b_k)$ and MAI. The mapping function of single user is

$$\begin{aligned} M(b_k) &= a_k a_k r_{kk} b_k - a_k y_k \\ &= a_k a_k r_{kk} b_k - a_k (a_k r_{kk} d_k + n_k). \end{aligned} \tag{19}$$

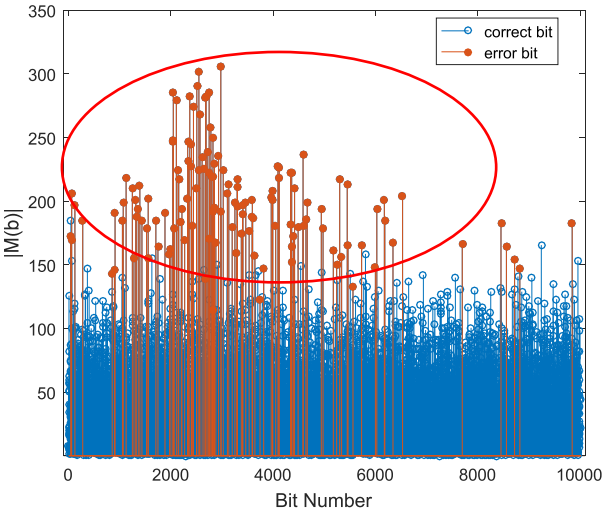

FIGURE 2. The absolute values of mapping function with $K = 10$ and SNR = 10dB.

For simplicity, we assume $a_k = 1$. The mapping function of the kth user in the multiuser environment is

$$\begin{aligned} M(b_k) &= \sum_{i=1}^{K} a_k a_i r_{ki} b_i - a_k y_k \\ &= r_{kk} b_k - (r_{kk} d_k + \sum_{\substack{i=1 \\ i\neq k}}^{K} r_{ki} d_i - \sum_{\substack{i=1 \\ i\neq k}}^{K} r_{ki} b_i + n_k), \end{aligned} \tag{20}$$

where b_i is the ith received bit and d_i is the transmitted bit of ith user. Comparing (20) with (19), the mapping function of multiuser has an extra term

$$\sum_{\substack{i=1 \\ i\neq k}}^{K} r_{ki} d_i - \sum_{\substack{i=1 \\ i\neq k}}^{K} r_{ki} b_i. \tag{21}$$

The extra term owing to MAI causes the change of the mapping value in Fig. 2. Note that the mapping function is affected by MAI and AWGN. In the condition of low SNR, AWGN is the main interference which is difficult to be suppressed, while in the condition of high SNR, MAI becomes the main effect instead of AWGN. We mainly consider MAI suppression and distinguish error bits affected by MAI. The ranges of mapping function in the multiuser environment can be discussed as follows.

A. ASSUME THAT $b_k = +1$

1) If the information bit $d_k = +1$, the kth user receive a correct bit, i.e., $d_k = +1 \rightarrow b_k = +1$.

Status 1: The error bit received in the single user environment without MAI turns to correct bit in the multiuser environment owing to the effect of MAI, i.e., MAI affects the judgment of received bit.

Condition 1: According to (8), the judgment of kth sign detector in the single user environment can be expressed as

$$y_k = r_{kk} + n_k < 0. \tag{22}$$

Algorithm 1 The Proposed Mapping-Based MUD

1: Begin Initialization $k = 1$
2: Receive the vector $\mathbf{b}$ by using (12)
3: **repeat**
4: Calculate $M(b_k)$ by using (20)
5: **if** $b_k = +1$
Calculate the range in status 3,
(a) $r_{kk} - \sum_{\substack{j=1 \\ j\neq k}}^{K} r_{kj}d_j + \sum_{\substack{j=1 \\ j\neq k}}^{K} r_{kj}b_j < M < r_{kk} + \sum_{\substack{j=1 \\ j\neq k}}^{K} r_{kj}b_j$
else
Calculate the range in status 7,
(b) $-r_{kk} + \sum_{\substack{j=1 \\ j\neq k}}^{K} r_{kj}b_j < M < -r_{kk} - \sum_{\substack{j=1 \\ j\neq k}}^{K} r_{kj}d_j + \sum_{\substack{j=1 \\ j\neq k}}^{K} r_{kj}b_j$
end
6: **if** $M(b_k)$ falls into the range (a) or (b)
goto 7
else
goto 8
end
7: Invert the sign of b_k
8: Let $k = k + 1$
9: **until** $k > K$

Condition 2: The judgment of kth sign detector in the multiuser environment is opposite to that in the single user environment, i.e.,

$$y_k = r_{kk} + \sum_{\substack{j=1 \\ j\neq k}}^{K} r_{kj}d_j + n_k > 0. \tag{23}$$

Combining (22), (23) and (20), the range of mapping function in status 1 can be expressed as

$$r_{kk} - \sum_{\substack{j=1 \\ j\neq k}}^{K} r_{kj}d_j + \sum_{\substack{j=1 \\ j\neq k}}^{K} r_{kj}b_j < M(b_k) < r_{kk} + \sum_{\substack{j=1 \\ j\neq k}}^{K} r_{kj}b_j. \tag{24}$$

Status 2: MAI does not affect the judgment of received bit. And the received bits in both single user environment and multiuser environment are correct.

Condition 1: Considering the prerequisite $b_k = +1$, the judgment of kth sign detector in the single user environment is

$$y_k = r_{kk} + n_k > 0. \tag{25}$$

Condition 2: The judgment of kth sign detector in the multiuser environment is given by

$$y_k = r_{kk} + \sum_{\substack{j=1 \\ j\neq k}}^{K} r_{kj}d_j + n_k > 0. \tag{26}$$

Then, the range of mapping function in status 2 can be derived as

$$M(b_k) < r_{kk} - \sum_{\substack{j=1 \\ j\neq k}}^{K} r_{kj}d_j + \sum_{\substack{j=1 \\ j\neq k}}^{K} r_{kj}b_j. \tag{27}$$

2) If the information bit $d_k = -1$, the kth user receive a error bit, i.e., $d_k = -1 \rightarrow b_k = +1$.

Status 3: The received bit in the single user environment is correct, moreover, the received bit in the multiuser environment is error owing to MAI.

Condition 1: According to the condition of $d_k = -1$, the judgment in the single user environment is

$$y_k = -r_{kk} + n_k < 0. \tag{28}$$

Condition 2: The judgment in the multiuser environment is opposite to that in the single user environment, i.e.,

$$y_k = -r_{kk} + \sum_{\substack{j=1 \\ j\neq k}}^{K} r_{kj}d_j + n_k > 0. \tag{29}$$

Here is the range of mapping function in status 3.

$$r_{kk} - \sum_{\substack{j=1 \\ j\neq k}}^{K} r_{kj}d_j + \sum_{\substack{j=1 \\ j\neq k}}^{K} r_{kj}b_j < M(b_k) < r_{kk} + \sum_{\substack{j=1 \\ j\neq k}}^{K} r_{kj}b_j. \tag{30}$$

Status 4: The received bit in the single user environment is error, the same as the situation in the multiuser environment.

Condition 1: The judgment in the single user environment is

$$y_k = -r_{kk} + n_k > 0. \tag{31}$$

Condition 2: The judgment in the multiuser environment is

$$y_k = -r_{kk} + \sum_{\substack{j=1 \\ j\neq k}}^{K} r_{kj}d_j + n_k > 0. \tag{32}$$

The range of mapping function can be given as

$$M(b_k) < r_{kk} - \sum_{\substack{j=1 \\ j\neq k}}^{K} r_{kj}d_j + \sum_{\substack{j=1 \\ j\neq k}}^{K} r_{kj}b_j. \tag{33}$$

B. ASSUME THAT $b_k = -1$

The analysis in section B is similar to that in section A. We can also obtain the ranges of mapping function in status 5, 6, 7 and 8. To avoid repetition, they are not described in this section. Finally, we summarize the results in Table 1.

The different status including all circumstances of MAI effect is shown in Table 1 along with the involved ranges of mapping function. Note that: a) In status 1, 3, 5 and 7, the judgment of received bit in the single user environment without MAI is opposite to that in the multiuser environment with MAI. In other words, the judgment of bit is affected

TABLE 1. The ranges of mapping function.

Status	d_k	b_k without MAI effect	b_k with MAI effect	The Ranges of Mapping Function
1	+1	-1	+1	$r_{kk} - \sum_{\substack{j=1 \\ j\neq k}}^{K} r_{kj} d_j + \sum_{\substack{j=1 \\ j\neq k}}^{K} r_{kj} b_j < M(b_k) < r_{kk} + \sum_{\substack{j=1 \\ j\neq k}}^{K} r_{kj} b_j$
2	+1	+1	+1	$M(b_k) < r_{kk} - \sum_{\substack{j=1 \\ j\neq k}}^{K} r_{kj} d_j + \sum_{\substack{j=1 \\ j\neq k}}^{K} r_{kj} b_j$
3	-1	-1	+1	$r_{kk} - \sum_{\substack{j=1 \\ j\neq k}}^{K} r_{kj} d_j + \sum_{\substack{j=1 \\ j\neq k}}^{K} r_{kj} b_j < M(b_k) < r_{kk} + \sum_{\substack{j=1 \\ j\neq k}}^{K} r_{kj} b_j$
4	-1	+1	+1	$M(b_k) < r_{kk} - \sum_{\substack{j=1 \\ j\neq k}}^{K} r_{kj} d_j + \sum_{\substack{j=1 \\ j\neq k}}^{K} r_{kj} b_j$
5	-1	+1	-1	$-r_{kk} + \sum_{\substack{j=1 \\ j\neq k}}^{K} r_{kj} b_j < M(b_k) < -r_{kk} - \sum_{\substack{j=1 \\ j\neq k}}^{K} r_{kj} d_j + \sum_{\substack{j=1 \\ j\neq k}}^{K} r_{kj} b_j$
6	-1	-1	-1	$M(b_k) > -r_{kk} + \sum_{\substack{j=1 \\ j\neq k}}^{K} r_{kj} b_j - \sum_{\substack{j=1 \\ j\neq k}}^{K} r_{kj} d_j$
7	+1	+1	-1	$-r_{kk} + \sum_{\substack{j=1 \\ j\neq k}}^{K} r_{kj} b_j < M(b_k) < -r_{kk} - \sum_{\substack{j=1 \\ j\neq k}}^{K} r_{kj} d_j + \sum_{\substack{j=1 \\ j\neq k}}^{K} r_{kj} b_j$
8	+1	-1	-1	$M(b_k) > -r_{kk} + \sum_{\substack{j=1 \\ j\neq k}}^{K} r_{kj} b_j - \sum_{\substack{j=1 \\ j\neq k}}^{K} r_{kj} d_j$

by MAI, no matter whether the effect of MAI is adverse or beneficial. It is obvious that the effect of MAI in status 3 and 7 is adverse to the BER performance. Meanwhile, the effect of MAI in status 1 and 5 offset the other interference, especially AWGN, revising the error bit. b) In status 2, 4, 6 and 8, MAI does not influence the judgment of received bit which is mainly influenced by AWGN. The MUD algorithms are not suitable for these four cases. Hence, the error bits in status 4 and 8 cannot be distinguished and revised. Furthermore, the range of mapping function in status 1 is the same as that in status 3. And the ranges in status 5 and status 7 are identical. We take status 1 and 3 as an example to analyze the relation between MAI and the range of mapping function. The analysis of status 5 and 7 is similar to status 1 and 3. If the value of mapping function falls into the range in status 1 and 3, we consider the received bit in the multiuser environment as an error bit seriously affected by MAI. Then, we can revise the bit by inverting the sign. However, the effect of MAI in status 1 is beneficial to the systems. In the condition of low SNR, MAI in status 1 can influence the proposed algorithm due to the improper revising. Nevertheless, the received bit is mainly affected by AWGN rather than MAI at low SNR. The effect of MAI cannot offset that of AWGN most of the time. On the other hand, the effect of AWGN can be ignored at high SNR. The number of bits belonging to status 1 is too small to influence the results of the proposed algorithm. Consequently, we can ignore the status 1 and status 5 to develop the proposed MUD algorithm, no matter whether SNR is high or low.

After analyzing the relation between MAI and the range of mapping function, we provide a realization of the proposed MUD algorithm shown in Algorithm 1. The MUD algorithm is based on the mapping function which can calculate the boundaries in different status. In order to calculate the range of mapping function, we consider the output of a suboptimal multiuser detector as d_j with the prerequisite of perfect channel estimation. The output of suboptimal multiuser detectors is approximate to information bits. Considering computational complexity and the BER performance, the demands for suboptimal multiuser detectors should be low complexity, the good BER performance and broad application range. A block diagram of the proposed joint multiuser detector is shown in Fig. 3. We combine the suboptimal detector with the proposed MUD algorithm. The output b_j^* of the suboptimal detector, such as the DEC or MMSE detector, is employed as real information bits.

Note that the computational complexity of the proposed joint MUD scheme is much lower than that of OMD. It is obvious that the suboptimal algorithm is a linear relationship with user number K. Moreover, the mapping-based MUD algorithm is also linear with respect to K^2 due to the realization of the algorithm. Hence, the joint MUD scheme has low computational complexity after being combined with a suboptimal detector.

IV. SIMULATION RESULTS AND ANALYSIS

In this section, the proposed joint MUD scheme based on the optimal mapping function and suboptimal detectors is applied to an asynchronous multiuser BPSK WDMA-UWB system for WSNs. We evaluate the performance of the proposed algorithm compared with the RAKE receiver with MRC scheme and 10 fingers, the traditional DEC and MMSE detectors, and

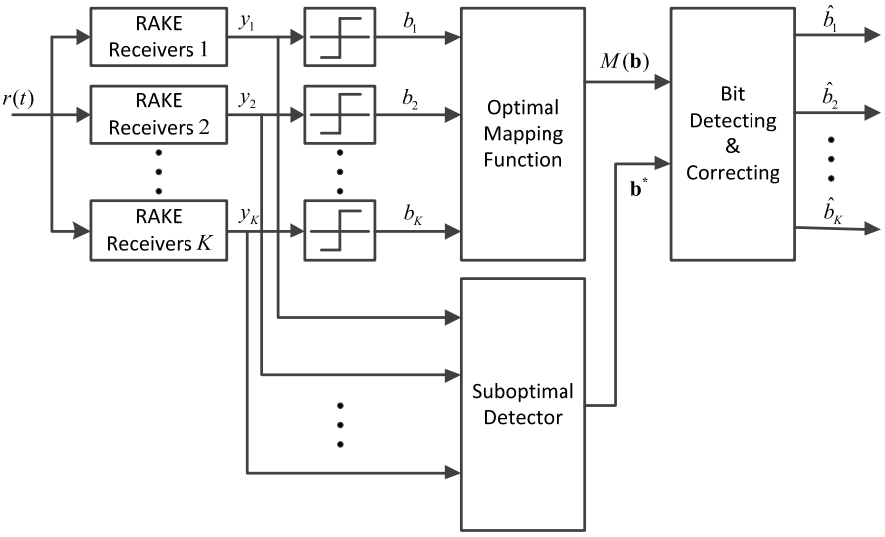

FIGURE 3. A block diagram of the joint detector based on optimal mapping function and suboptimal detector.

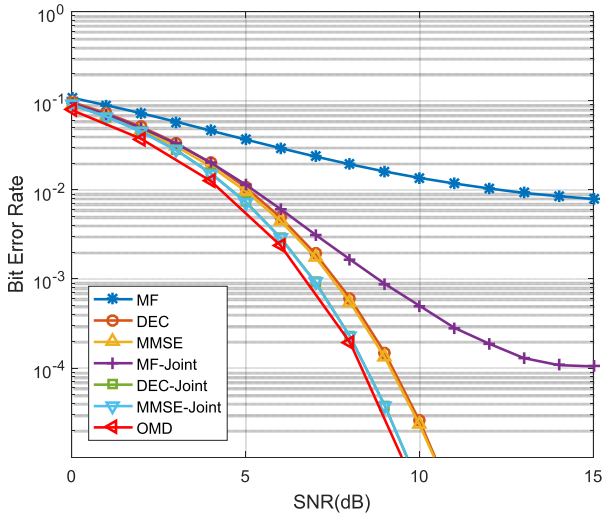

FIGURE 4. BER performance of various receivers with user number $K = 10$.

the OMD detector under the assumption of perfect channel estimation. Note that the Gegenbauer pulse waveforms with the pulse width of 1 ns described in Section II are adopted in the UWB system to suppress MAI in transmitters. The Gegenbauer waveforms are generated for each user with the coefficient $\gamma = 4$. The repetition period of per pulse T_s is 50 ns to avoid ISI. We consider the channel model 2 (CM2) standard of IEEE 802.15.4a channel modes, which is for indoor NLOS environments with a range from 7-20 m [24] and suitable for indoor WSNs.

In the first set of simulations, we assume that all the users transmit at the equal power. We evaluate the BER performance of the proposed MUD scheme that is introduced in Section III. Fig. 4 shows the BER performance of proposed algorithm with 10 users. The curve marked OMD is the BER performance of the optimal multiuser detector, which is the theoretical lower limit of BER for multiuser UWB systems. The 10-finger RAKE receiver is able to utilize the multipath energy to suppress multipath interference which can get limited improvement of the multiple access performance. The traditional DEC and MMSE detectors can suppress MAI effectively in this simulation and have essentially the same BER performance. Moreover, we consider the output of MF, DEC and MMSE receivers as the real information bits, respectively, calculating the ranges of mapping function to realize the proposed algorithm. The curves of these joint detectors are shown in this figure. Note that the performance of the MF-joint receiver is poor owing to the high BER of the MF detector. However, the DEC-joint and MMSE-joint receivers have a superior BER performance close to the OMD detector compared with the others.

Figs. 5-8 depict the BER performance of various detectors for 20, 30, 40 and 50 users, respectively. The performance of DEC-joint and MMSE-joint receivers in Fig. 5 is almost the same as that in Fig. 4, and in Fig. 6 the two joint receivers show at most 1dB degradation in the performance. It is obvious in Fig. 4-8 that the receivers exhibit gradual performance degradation as the number of user increase. Note that the MMSE-joint receiver has a better performance than the DEC-joint receiver in Fig. 7 when the user number increases to 40. Compared with the MMSE-joint receiver, the DEC-joint has about 2dB performance degradation when the user number is 50 due to the worse performance of the DEC detector. Hence, we suggest using the MMSE-joint receiver to suppress MAI.

The user number and the performance of suboptimal detectors are two important factors which can influence the BER performance. In Fig. 9, the BER performance at SNR = 6dB for different user number from 10 to 50 is illustrated. Due to the increasing user number, the effect of MAI and multipath interference is more and more serious. Hence, the performance of DEC and MMSE receivers become deteriorated.

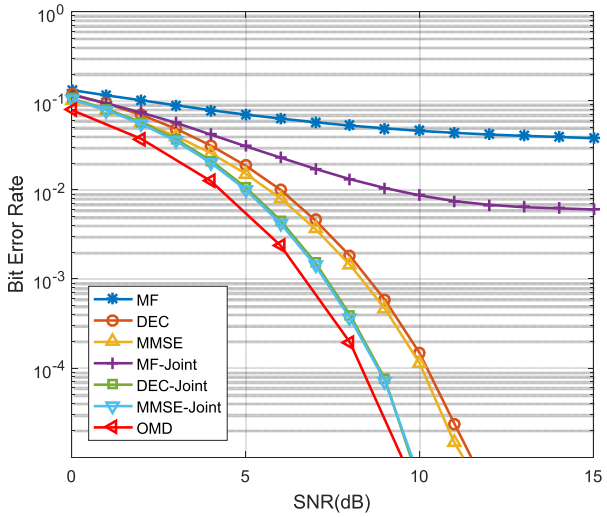

FIGURE 5. BER performance of various receivers with user number $K = 20$.

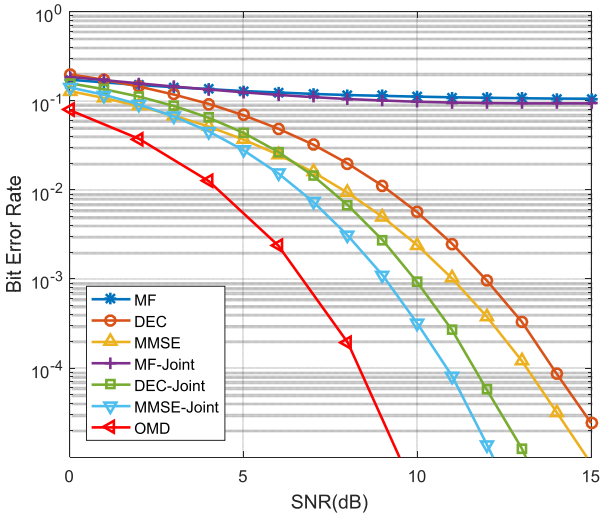

FIGURE 7. BER performance of various receivers with user number $K = 40$.

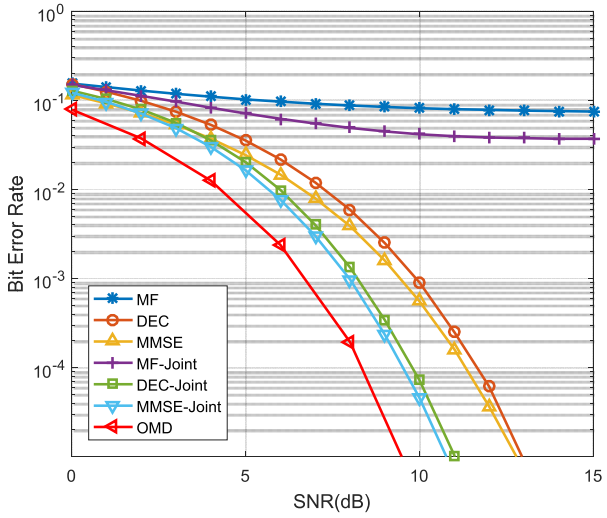

FIGURE 6. BER performance of various receivers with user number $K = 30$.

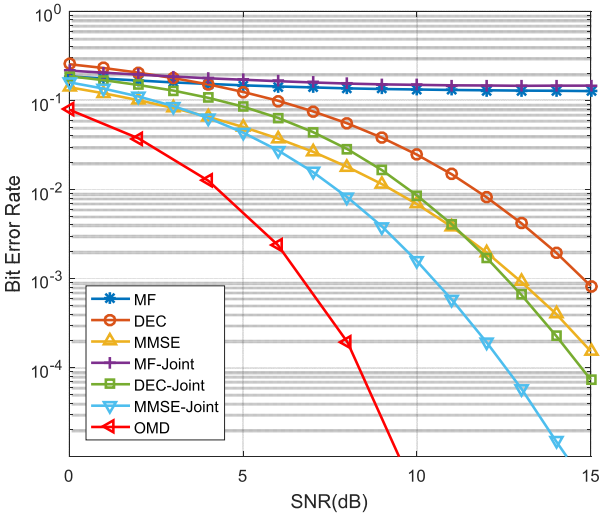

FIGURE 8. BER performance of various receivers with user number $K = 50$.

It is obvious that the DEC detector is more sensitive to user number than the MMSE receiver. Moreover, the MMSE-joint receiver is subject to the performance of the MMSE detector. Consequently, the MMSE-joint receiver's performance deteriorates slightly as the number of users increases. But the MMSE-joint receiver is consistently the best receiver among all the MUD detectors. The performance of suboptimal detectors is another important factor which can influence the proposed algorithm. As is shown in Fig. 9, the deterioration of MMSE and DEC detectors may affect the BER performance of the joint detector. In order to solve this problem, we present a duple joint detection method shown in Fig. 10. The curve marked 1st-Joint is the MMSE-joint receiver in Fig. 8. After detecting all the received bits, we consider the output of the MMSE-joint receiver as the real information bits. Due to the better performance of the MMSE-joint receiver than that of the MMSE receiver, the second joint detection can achieve lower BER which is shown as the curve marked 2nd-Joint. The second joint detection has about 0.5dB improvement. The simulation result accords with the previous analysis and we can use the duple joint detection method to achieve a better performance. However, we cannot improve the BER performance with no limit. The improvement becomes indistinct along with the increasing times of joint detection.

The proposed joint MUD scheme is suitable for small UWB-based WSNs without power control. In such networks, the received power from interfering users can be tens of dB larger than the desired signals which result in a near-far problem. Thus, the near–far resistance is a common performance measure for analyzing UWB systems. We consider a 10-user WDMA-UWB system where near-far interference effect is present. Assume that the user 1 is the desired user and user 2-10 are interfering users. The desired

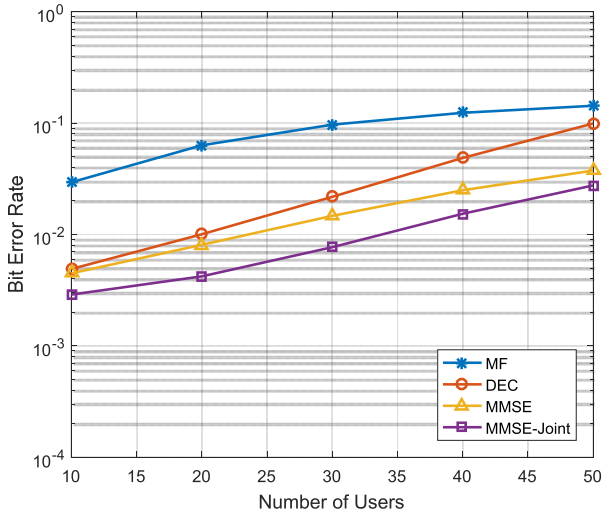

FIGURE 9. BER performance at SNR = 6dB for different number of users.

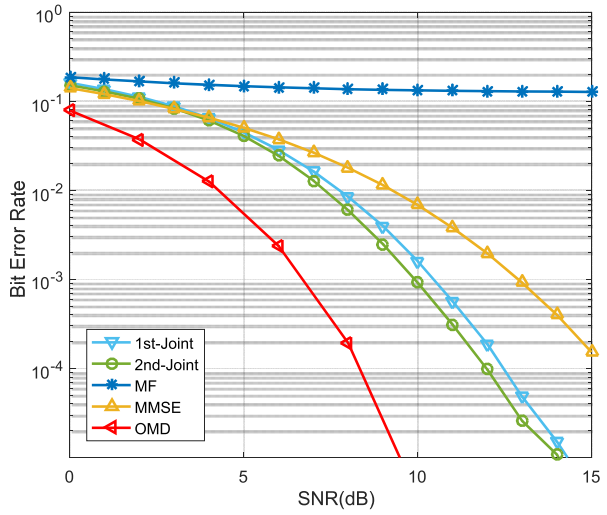

FIGURE 10. BER performance of duple joint detection method with user number $K = 50$.

user's SNR is fixed on 5dB. The SNR of other users varies from 0dB to 15dB synchronously. Fig. 11 shows the near-far resistance of different receivers. Note that the performance of MF detector is very poor due to the presence of near-far interference. Moreover, the DEC and MMSE receivers are unaffected by the near-far effect. Due to the good near-far resistance performance of the MMSE receiver, the proposed MMSE-joint detector has a good BER performance approximating to that of the OMD detector. The simulation results demonstrate that the proposed joint MUD scheme can counteract the near-far interference effectively.

It is obvious that the OMD algorithm has the best performance with exponential complexity. Meanwhile, the suboptimal MUD receivers which are combined with the proposed MUD scheme are traditional linear MUD receivers. In order to show that the computational complexity of the proposed joint MUD scheme is low and not exponentially with the number of users, we calculate the times of addition

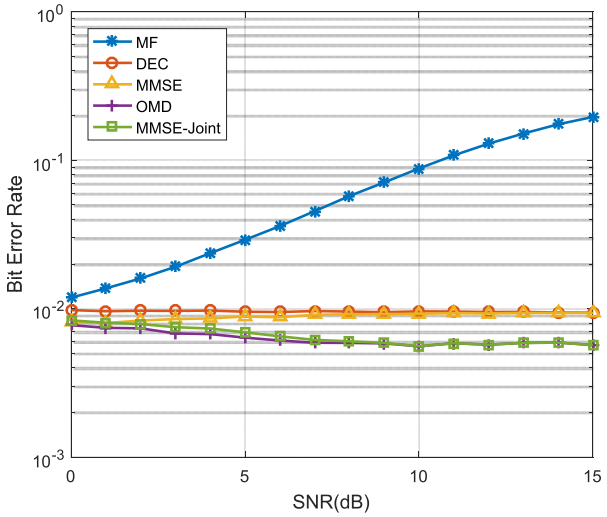

FIGURE 11. Near–far resistance of various receivers with 10 users at SNR = 5dB of desired user. The other users have the same SNR varying from 0dB to 15dB.

operation and multiplication operation respectively to assess the complexity. According to the realization of the proposed algorithm, the addition and multiplication have almost the same times $K(2K + 2)$, where K is the number of users. The computational complexity of the proposed MUD scheme can be expressed as $O(K^2)$. By contrast, the computational complexity of the OMD algorithm is equivalent to $O(2^K)$. Therefore, the complexity of the proposed joint scheme is much lower than that of the OMD algorithm. Besides, the proposed joint MUD scheme performs better than all other suboptimal MUD receivers with slightly higher computational complexity.

V. CONCLUSION

In this paper, a joint MUD scheme for WDMA-UWB communication systems was proposed. Gegenbauer orthogonal pulses assigned to different users were adopted to realize WDMA technology which has higher data rate and simpler transceivers. The joint MUD scheme was derived based on the optimal mapping function and suboptimal detectors. The mapping function was employed to map the received bits into the mapping space and subsequently the ranges of the mapping function in different status was analyzed to distinguish error bits affected by MAI. Suboptimal detectors were combined with the proposed MUD algorithm to calculate the boundaries of error bits in the mapping space. Simulation results showed that the MMSE-joint MUD receiver performed better than DEC-joint receiver and other suboptimal detectors. Duple joint detection method can be used to obtain limited improvement. Also, the near-far resistance performance of the MMSE-joint receiver outperformed that of all other suboptimal receivers. Moreover, the computational complexity of the proposed joint scheme is much lower than that of the OMD algorithm. Therefore, the proposed joint MUD scheme can be regarded as a promising solution for WDMA-UWB WSNs.

REFERENCES

[1] T. Liu, T. Gu, N. Jin, and Y. Zhu, "A mixed transmission strategy to achieve energy balancing in wireless sensor networks," *IEEE Trans. Wireless Commun.*, vol. 16, no. 4, pp. 2111–2122, Apr. 2017.
[2] K. Han, J. Luo, Y. Liu, and A. V. Vasilakos, "Algorithm design for data communications in duty-cycled wireless sensor networks: A survey," *IEEE Commun. Mag.*, vol. 51, no. 7, pp. 107–113, Jul. 2013.
[3] H. I. Kobo, A. M. Abu-Mahfouz, and G. P. Hancke, "A survey on software-defined wireless sensor networks: Challenges and design requirements," *IEEE Access*, vol. 5, pp. 1872–1899, 2017.
[4] F. Lazzari, A. Buffi, P. Nepa, and S. Lazzari, "Numerical investigation of an UWB localization technique for unmanned aerial vehicles in outdoor scenarios," *IEEE Sensors J.*, vol. 17, no. 9, pp. 2896–2903, Sep. 2017.
[5] Q. Fan, B. Sun, Y. Sun, and X. Zhuang, "Performance enhancement of MEMS-based INS/UWB integration for indoor navigation applications," *IEEE Sensors J.*, vol. 17, no. 10, pp. 3116–3130, May 2017.
[6] V. Henriques and R. Malekian, "Mine safety system using wireless sensor network," *IEEE Access*, vol. 4, pp. 2169–3536, 2016.
[7] K. Bai and C. Tepedelenlioglu, "Distributed detection in UWB wireless sensor networks," *IEEE Trans. Signal Process.*, vol. 58, no. 2, pp. 804–813, Feb. 2010.
[8] Q. Z. Ahmed, L. L. Yang, and S. Chen, "Reduced-rank adaptive least bit-error-rate detection in hybrid direct-sequence time-hopping ultrawide bandwidth systems," *IEEE Trans. Wireless Commun.*, vol. 60, no. 3, pp. 849–857, Apr. 2010.
[9] C. S. Sum, S. Sasaki, and H. Harada, "Impact of chip duty factor on DS, TH and DS-TH UWB systems in realistic environment," *IEICE Trans. Fund. Electron. Commun. Comput. Sci.*, vol. 93, no. 10, pp. 1716–1723, Oct. 2010.
[10] N. Zhao, X. W. Lv, and Z. L. Wu, "A hybrid ant colony optimization algorithm for optimal multiuser detection in DS-UWB system," *Exp. Syst. Appl.*, vol. 39, no. 5, pp. 5279–5285, Sep. 2012.
[11] H.-L. Hung, Y.-F. Huang, and C.-H. Cheng, "Performance of hybrid Hopfield neural networks with EM algorithms for multiuser detection in ultra-wide-band communication systems," in *Proc. IEEE Int. Conf. Syst., Man, Cybern.*, New York, NY, USA, Sep. 2011, pp. 1423–1429.
[12] Z. L. Wu, Z. Y. Zong, and Z. D. Yin, "Joint multiuser detection of CD and AFSA in DS-UWB communication systems," *Inf. Technol. J.*, vol. 10, no. 2, pp. 422–427, 2011.
[13] Z. Zong, Z. Yin, and Z. Wu, "The population declining AFSA based identification of active users for cooperative cognitive radio networks with DS-UWB based control channel," in *Proc. 8th Int. Conf. Wireless Commun., Netw. Mobile Comput. (WiCOM)*, Sep. 2012, pp. 1–5.
[14] N. Zhao, Z. Wu, Y. Zhao, and T. Quan, "A population declining mutated ant colony optimization multiuser detector for MC-CDMA," *IEEE Commun. Lett.*, vol. 14, no. 6, pp. 497–499, Jun. 2010.
[15] N. I. Miridakis, D. D. Vergados, "Complexity analysis of a hybrid threshold-based ZF-MMSE equalizer for sic-based MIMO-OFDM receivers," in *Proc. Int. Conf. Wireless Inf. Netw. Syst.*, 2011, pp. 109–112.
[16] Z. Y. Y. Kuang, H. Sun, Z. Wu, and W. Tang, "A hybrid multiuser detection algorithm for outer space DS-UWB ad-hoc network with strong narrowband interference," *Ksii Trans. Int. Inf. Syst.*, vol. 6, no. 5, pp. 1316–1332, May 2012.
[17] P. Kaligineedi and V. K. Bhargava, "Frequency-domain turbo equalization and multiuser detection for DS-UWB systems," *IEEE Trans. Wireless Commun.*, vol. 7, no. 9, pp. 3280–3284, Sep. 2008.
[18] M. Jayasheela, A. Rajeswari, and D. Prabha, "Multi-user detection schemes for TH PPM UWB system using LDPC codes," *Int. J. Comput. Appl.*, vol. 38, no. 11, pp. 40–41, 2012.
[19] Z. Yin, Z. Wang, X. Liu, and Z. Wu, "Design of pulse waveform for waveform division multiple access UWB wireless communication system," *Sci. World J.*, vol. 2014, no. 2, pp. 1–11, 2014.
[20] Z. Yin, S. Wu, Z. Shi, and Z. Wu, "A new design of pulse waveform for waveform division multiple access UWB wireless communication system," in *Proc. 8th IEEE Int. Conf. Commun. Softw. Netw.*, Beijing, China, Apr. 2016, pp. 535–538.
[21] L. Sakkila, A. Rivenq, and C. Tatkeu, "Comparison of classical and orthogonal UWB waveforms for radar applications," in *Proc. 6th Int. Colloq. Signal Process. Appl.*, Malacca, Malaysia, 2010, pp. 1–5.
[22] F. Elbahhar, A. Rivenq-Menhaj, and J. M. Rouvaen, "Multi-user ultra-wide band communication system based on modified gegenbauer and Hermite functions," *Wireless Person. Commun.*, vol. 34, no. 3, pp. 255–277, Mar. 2005.
[23] A. F. Molisch, *et al.*, "IEEE 802.15.4a channel model-Final report," IEEE 802.15 SG4a, NY, USA, Tech. Rep. IEEE 802.15-0400662-02-004a, 2004.
[24] A. F. Molisch *et al.*, "A comprehensive standardized model for ultrawideband propagation channels," *IEEE Trans. Antennas Propag.*, vol. 54, no. 11, pp. 3151–3166, Nov. 2006.

ZHENDONG YIN received the Ph.D. degree from Harbin Institute of Technology (HIT), Harbin, China in 2008. He is currently an Associate Professor with the School of Electronics Information Engineering, HIT. His current research interests are UWB wireless communication, formation flying satellites communication, and relay satellite system.

MINGYANG WU received the B.Sc. and M.Sc. degrees in information and communication engineering from the School of Electronics and Information Engineering, Harbin Institute of Technology (HIT), Harbin, China, in 2013 and 2016, respectively. He is currently pursuing the Ph.D. degree with HIT. His research interests include UWB wireless communication, signal processing algorithms, and MIMO technology.

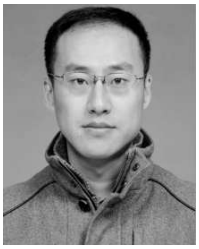

ZHUTIAN YANG received the M.E. and Ph.D. degrees from the Harbin Institute of Technology (HIT), Harbin, China, in 2008 and 2013, respectively. He was a Visiting Research Associate with King's College London, U.K., in 2015. He is currently an Associate Professor with HIT. His general research interests include smart communication technology, signal processing algorithms, and machine learning.

NAN ZHAO (S'08–M'11–SM'16) received the B.S. degree in electronics and information engineering, the M.E. degree in signal and information processing, and the Ph.D. degree in information and communication engineering from the Harbin Institute of Technology, Harbin, China, in 2005, 2011, and 2007, respectively. From 2011 to 2013, he was with the Dalian University of Technology, Dalian, China, where he was involved in postdoctoral research. He is currently an Associate Professor with the School of Information and Communication Engineering, Dalian University of Technology. His recent research interests include interference alignment, cognitive radio, wireless power transfer, and physical layer security.

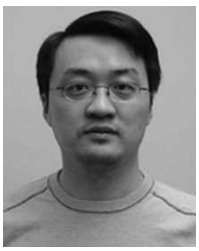

YUNFEI CHEN (S'02–M'06–SM'10) received the B.E. and M.E. degrees in electronics engineering from Shanghai Jiaotong University, Shanghai, China, in 1998 and 2001, respectively, and the Ph.D. degree from the University of Alberta, Edmonton, AB, Canada, in 2006. He is currently an Associate Professor with the University of Warwick, U.K. His research interests include wireless communications, cognitive radios, wireless relaying, and energy harvesting.